1-1-2008

Preliminary Integrated Chronostratigraphy of the AND-2A Core, ANDRILL Southern McMurdo Sound Project, Antarctica

G. Acton
University of California - Davis, gdacton@ucdavis.edu

J. Crampton
GNS Science

G. Di Vincenzo
Istituto di Geoscienze e Georisorse

Christopher R. Fielding
University of Nebraska-Lincoln, cfielding2@unl.edu

F. Florindo
Istituto Nazionale di Geofisica e Vulcanologia

See next page for additional authors

Authors
G. Acton, J. Crampton, G. Di Vincenzo, Christopher R. Fielding, F. Florindo, M. Hannah, D. M. Harwood, S. Ishman, K. Johnson, L. Jovane, Richard Levy, B. Lum, M. C. Marcano, S. Mukasa, C. Ohneiser, M. P. Olney, C. Riesselman, L. Sagnotti, C. Stefano, E. Strada, M. Taviani, E. Tuzzi, K. L. Verosub, G. S. Wilson, M. Zattin, and ANDRILL-SMS Science Team

Terra Antartica
2008-2009, **15**(1), 211-220

Preliminary Integrated Chronostratigraphy of the AND-2A Core, ANDRILL Southern McMurdo Sound Project, Antarctica

G. Acton[1*], J. Crampton[2], G. Di Vincenzo[3], C.R. Fielding[4], F. Florindo[5], M. Hannah[6], D.M. Harwood[4,7], S. Ishman[8], K. Johnson[9], L. Jovane[1], R.H. Levy[7], B. Lum[1], M.C. Marcano[10], S. Mukasa[10], C. Ohneiser[11], M.P. Olney[12], C. Riesselman[13], L. Sagnotti[5], C. Stefano[10], E. Strada[5,14], M. Taviani[15], E. Tuzzi[4,16], K.L. Verosub[1], G.S. Wilson[11], M. Zattin[17] & the ANDRILL-SMS Science Team[18]

[1]Geology Department, University of California – Davis, One Shields Ave., Davis, CA, 95616 - USA
[2]GNS Science, 1 Fairway Drive, PO Box 30308, Lower Hutt - New Zealand
[3]Istituto di Geoscienze e Georisorse, CNR, Via Moruzzi 1, I-56124 Pisa - Italy
[4]Department of Geoscience, University of Nebraska-Lincoln, Lincoln, NE, 68588-0340 - USA
[5]Istituto Nazionale di Geofisica e Vulcanologia, Via di Vigna Murata, 605, I-00143 Rome - Italy
[6]School of Earth Sciences, Victoria University of Wellington, PO Box 600, Wellington 4007 - New Zealand
[7]ANDRILL Science Management Office, University of Nebraska-Lincoln, Lincoln, NE, 68588-0341 - USA
[8]Department of Geology, Southern Illinois University, 1259 Lincoln Drive, Carbondale, IL, 62901 - USA
[9]School of Earth Sciences, The Ohio State University, 125 South Oval Mall, Columbus, OH, 43210 - USA
[10] Dept. of Geological Sciences, University of Michigan, 1100 N. University Ave., Ann Arbor, MI, 48109 - USA
[11]Department of Geology, University of Otago, PO Box 56, Dunedin - New Zealand
[12]Department of Geology, University of South Florida, 4202 E. Fowler Ave., SCA 528, Tampa, FL, 33620 - USA
[13]Geological and Environmental Sciences, Stanford University, Braun Hall, Bldg. 320, Stanford, CA, 94305 - USA
[14]Dipartimento di Scienze della Terra, Università di Siena, Via del Laterino 8, I-53100 Siena – Italy
[15]CNR, ISMAR - Bologna, Via Gobetti 101, I-40129 Bologna - Italy
[16]Now at ExxonMobil Exploration Company, 233 Benmar Dr. Houston TX 77060
[17]Dip. Scienze della Terra e Geologico-Ambientali, Università di Bologna, Via Zamboni 67, I-40126 Bologna - Italy
[18]http://www.andrill.org/projects/sms/team.html

**Corresponding author* (gdacton@ucdavis.edu)

Abstract - We use all available chronostratigraphic constraints – biostratigraphy, magnetostratigraphy, radioisotopic dates, strontium-isotope stratigraphy, and correlation of compositional and physical properties to well-dated global or regional records – to construct a preliminary age model for ANDRILL SMS Project's AND-2A drillcore (77°45.488'S, 165°16.605'E, 383.57 m water depth). These diverse chronostratigraphic constraints are consistent with each other and are distributed throughout the 1138.54 m-thick section, resulting in a well-constrained age model. The sedimentary succession comprises a thick early and middle Miocene section below 224.82 mbsf and a condensed middle/late Miocene to Recent section above this. The youngest sediments are Brunhes age (<0.781 Ma), as confirmed by a radioisotopic age of 0.691±0.049 Ma at 10.23 mbsf and the occurrence of sediments that have normal magnetic polarity down to ~31.1 mbsf, which is interpreted to be the Brunhes/Matuyama reversal (0.781 Ma). The upper section is punctuated by disconformities resulting from both discontinuous deposition and periods of extensive erosion typical of sedimentary environments at the margin of a dynamic ice sheet. Additional breaks in the section may be due to the influence of tectonic processes. The age model incorporates several major hiatuses but their precise depths are still somewhat uncertain, as there are a large number of erosional surfaces identified within the stratigraphic section. One or more hiatuses, which represent a total 7 to 8 million years of time missing from the sedimentary record, occur between about 50 mbsf and the base of Lithostratigraphic Unit (LSU) 3 at 122.86 mbsf. Similarly, between about 145 mbsf and the base of LSU 4 at 224.82 mbsf, one or more hiatuses occur on which another 2 to 3 million years of the sedimentary record is missing. Support for the presence of these hiatuses comes from a diatom assemblage that constrains the age of the core from 44 to 50 mbsf to 2.06-2.84 Ma, two radioisotopic dates (11.4 Ma) and a Sr-isotope date (11.7 Ma) that indicate the interval from 127 to 145 mbsf was deposited between 11.4 and 11.7 Ma, and three diatom occurrence datums from between 225.38 and 278.55 mbsf that constrain the age of this upper part of Lithostratigraphic Unit (LSU) 5 to 14.29 - 15.89 Ma. Below the boundary between LSU 5 and 6 sedimentation was relatively continuous and rapid and the age model is well-constrained by 9 diatom datums, seven ^{40}Ar-^{39}Ar dates, one Sr-isotope date, and 19 magnetozones. Even so, short hiatuses (less than a few hundred thousand years) undoubtedly occur but are beyond the resolution of current chronostratigraphic age constraints. Diatom first and last occurrence datums provide particularly good age control from the top of LSU 6 down to 771.5 mbsf (in LSU 10), where the First Occurrence (FO) of *Thalassiosira praefraga* (18.85 Ma) is observed. The diatom datum ages are supported by radioisotopic dates of 17.30±0.31 Ma at 640.14 mbsf (in LSU 9) and 18.15±0.35 and 17.93±0.40 Ma for samples from 709.15 and 709.18 mbsf (in LSU 10), respectively, and 18.71±0.33 Ma for a sample from 831.67 mbsf (in LSU 11). The sediments from 783.69 mbsf to the base of the hole comprise two thick normal polarity magnetozones that bound a thinner reversed polarity magnetozone (958.59 - 985.64 mbsf). This polarity sequence most likely encompasses Chrons C5En, C5Er, and C6n (18.056 - 19.772 Ma or slightly older given uncertainties in this section of the geomagnetic polarity timescale), but could be also be Chrons C6n, C6r, and C6An.1n (18.748 - 20.213 Ma). Either polarity sequence is compatible with the ^{40}Ar–^{39}Ar age of 20.01±0.35 Ma obtained from single-grain analyses of alkali feldspar from a tephra sample from a depth of 1093.02 mbsf, although the younger interpretation allows a better fit with chronostratigraphic data up-core. Given this age model, the mean sedimentation rate is about 18 cm/k.y. from the top of LSU 6 to the base of the hole.

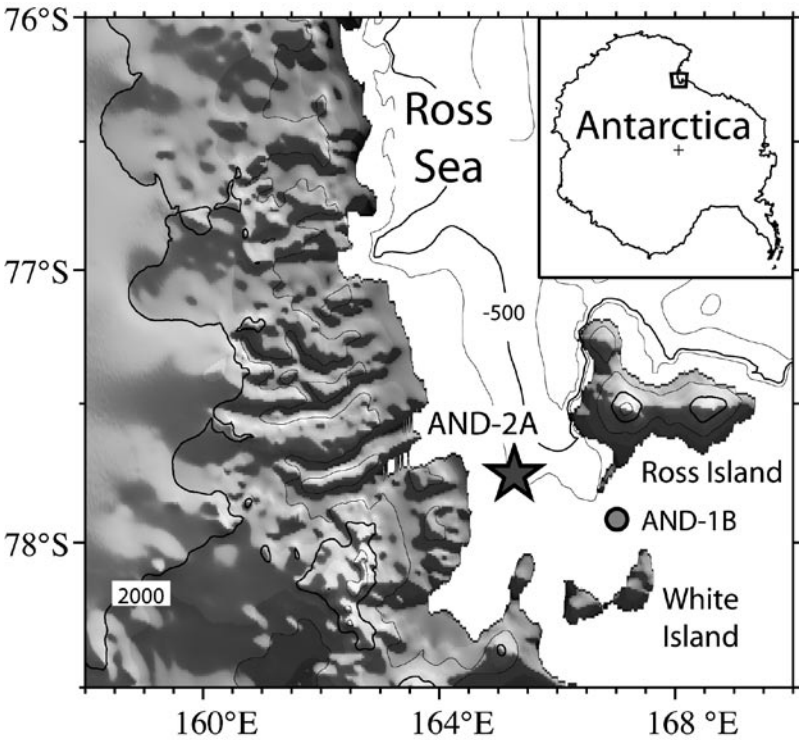

Fig. 1 - A Mercator relief map with contours showing the location of the AND-2A and AND-1B drill sites. Contour intervals are every 250 m for the bathymetry (ETOPO2 bathymetry data from the National Geophysical Data Center at http://www.ngdc.noaa.gov/mgg/global/global.html) and every 1000 m for the topography (GTOPO30 topography data from the United States Geological Survey at http://edc.usgs.gov/products/elevation/gtopo30/gtopo30.html). The small box in the inset shows the main map location relative to Antarctica. The maps were made using GMT software (Wessel and Smith, 1998).

INTRODUCTION

ANDRILL's Southern McMurdo Sound (SMS) Project cored Hole AND-2A (77°45.488'S, 165°16.605'E, ~383.57 m water depth) to a total depth of 1138.54 mbsf and recovered over a kilometer of core (Fig. 1). The goal of this chronostratigraphy report is to integrate all age information available as of September 2008 into a coherent age model for the AND-2A core. Currently, the age model incorporates data from biostratigraphy and magnetostratigraphy studies, radioisotopic dating of volcaniclastic sediments and tephras, $^{87}Sr/^{86}Sr$ dating of micro- and macrofossils, and correlation of compositional and physical properties to well-dated global or regional records. This age model provides a basis for studying the timing and rates of geologic, climatic, and tectonic events recorded in the core, and for comparing them with other records from around the world.

Because new age constraints are still being obtained as part of the 'Science Documentation' phase of the ANDRILL-SMS Project, the age model is considered to be preliminary. A revised age model will be constructed in the future that uses the data presented here and incorporates new age information from the Science Documentation phase. Important age constraints may come from any of the many disciplines involved in the ANDRILL-SMS Project and, hence, the age model is necessarily a group effort that will continue to evolve.

CHRONOSTRATIGRAPHIC DATA

Primary chronostratigraphic constraints available at present include marine diatom datums and radioisotopic dates, which together are relatively evenly distributed throughout the stratigraphic section (Tab. 1). The independently derived ages provided by these two methods agree well with each other. Magnetic polarity zones (magnetozones) complement and aid in refining the age constraints particularly in Lithostratigraphic Units (LSU) 8 through 14, which span from 436.18 mbsf to the bottom of

Tab. 1 - Age data for core AND-2A.

Young Age (Ma)	*Old Age (Ma)*	*Age Used (Ma)*	*Top Depth (mbsf)*	*Bottom Depth (mbsf)*	*Depth (mbsf)*	*Sed rate (cm/k.y.)*	*Description*	*Data Type*
AGE MODEL (Solid curve in Figure 1)								
0.000	0.000	0.000	0.000	0.000	0.000			
0.64	0.74	0.691	10.22	10.24	10.230	1.48	40Ar-39Ar date on a lava clast	
0.781	0.781	0.781	25.340	36.860	31.100	23.19	B/M Chron C1n(o)	
0.850	0.850	0.850	38.000	38.000	38.000	10.00	Model age	
			38.000	38.000			Hiatus	
2.370	2.370	2.370	38.000	38.000	38.000		Model age	
2.060	2.840	2.450	44.060	48.240	46.150	10.19	Diatom Assemblage	
2.485	2.485	2.485	50.000	50.000	50.000	11.00	Model age	
			50.000	122.860			Poor age constraints and one or more hiatuses	
11.300	11.300	11.300	122.860	122.860	122.860		Model age	
11.390	11.390	11.390	128.000	128.000	128.000	5.71	Interval constrained by two 40Ar/39Ar dates	
10.550	12.950	11.670	144.030	144.060	144.045	5.73	Interval constrained by Sr-isotope date	
							Weak age constraints and one or more hiatuses	
15.500	15.500	15.500	296.340	296.340	296.340		Model age at top of LSU 6 based on diatoms	
20.200	20.200	20.200	1138.54	1138.54	1138.540	17.92	Model age of oldest sediment	

the hole. Sr-isotopic dates further support these other age constraints. Relatively few age constraints are available in the upper 224.82 m of the section, which spans from within LSU 1 to the base of LSU 4. Within this interval, datable material is sparse and sedimentation is discontinuous, with the possibility of multiple hiatuses that are several million years in duration. Some of these hiatuses are suspected to be of regional extent and thus may correlate to hiatuses that have been dated at other drill sites, particularly if the hiatuses correspond to regional seismic reflectors.

Tab. 1 - Continued.

Young Age (Ma)	*Old Age (Ma)*	*Age Used (Ma)*	*Top Depth (mbsf)*	*Bottom Depth (mbsf)*	*Depth (mbsf)*	*Sed rate (cm/k.y.)*	*Description*	*Reversal Type*
AGES FROM MAGNETOSTRATIGRAPHY Preferred Interpretation								
		0.781	25.340	36.860	31.100	3.98	B/M	N/R
		16.268	412.00	414.52	413.26	2.47	C5Cn.1n(o)/C5Cn.1r(y)	N/R
		16.543	446.95	451.37	449.16	13.05	C5Cn.2r(o)/C5Cr.3n(y)	R/N
		16.721	486.68	489.74	488.21	21.94	C5Cn.3n(o)/C5Cr(y)	N/R
		17.235	579.05	583.63	581.34	18.12	C5Cr(o)/C5Dn(y)	R/N
		?	640.46	645.57	643.02		C5Dn-1r(y) = an Excursion in C5Dn	N/R
		?	646.08	646.68	646.38		C5Dn-1r(o) = an Excursion in C5Dn	R/N
		17.533	723.36	724.10	723.73	47.78	C5Dn(o)/C5Dr.1r(y)	N/R
		17.717	748.25	750.55	749.40	13.95	C5Dr.1r(o)/C5Dr.1n(y)	R/N
		17.740	757.08	761.42	759.25	42.83	C5Dr.1n(o)/C5Dr.2r(y)	N/R
		18.056	783.16	784.22	783.69	7.73	C5Dr.2r(o)/C5En(y)	R/N
		18.524	957.93	959.25	958.59	37.37	C5En(o)/C5Er(y)	N/R
		18.748	978.92	992.36	985.64	29.18	C5Er(o)/C6n(y)	R/N
		<19.772			1138.54	<15	Base of the hole assuming lowest magnetozone is C6n	
Alternate Interpretation								
		1.945	25.340	36.860	31.100	1.60	C2n(o)/C2r.1r(y)	N/R
		17.235	579.05	583.63	581.34	3.60	C5Cr(o)/C5Dn(y)	R/N
		17.533	640.46	645.57	643.02	20.70	C5Dn(o)/C5Dr.1r(y)	N/R
		18.056	646.08	646.68	646.38	0.64	C5Dr.2r(o)/C5En(y)	R/N
		18.524	723.36	724.10	723.73	16.53	C5En(o)/C5Er(y)	N/R
		18.748	783.16	784.22	783.69	26.77	C5Er(o)/C6n(y)	R/N
		19.772	957.93	959.25	958.59	17.08	C6n(o)/C6r(y)	N/R
		20.040	978.92	992.36	985.64	10.09	C6r(o)/C6An.1n(y)	R/N
		<20.213			1138.54	<88	Base of the hole assuming lowest magnetozone is C6An.1n	
AGES FROM DIATOMS								
		0.64			47.00		*T. elliptipora*	LAD
		2.06			48.22		*T. elliptipora*	FAD
		2.15			44.06		*T. vulnifica*	LAD
		2.20			45.05		*T. torokina*	LAD
		2.40			47.00		*A. maccollumii*	LAD
		2.53			47.00		*T. inura*	LAD
		2.84			48.24		*A. maccollumii*	FAD
2.060	2.550	2.305	44.060	48.240	46.150		Diatom Assemblage (LAD & FAD *T. elliptipora*, LAD *T. vulnifica*, LAD *T. torokina*, LAD & FAD *A. maccollumii*, and LAD *T. inura*)	Assem-blage
		3.18			49.83		*T. vulnifica*	FAD
		4.77			49.78		*T. inura*	FAD
		8.03			49.78		*T. torokina*	FAD
		12.46			234.15		*D. lauta sensu latu*	LAD
		14.20			225.38		Absence of *D. simonseni* below 225.38 mbsf	FAD
		14.29			225.38		*D. maccollumii*	LAD
		15.50			310.10		N. sp. 17 Schrader	LAD
		15.70			312.03		*D. lauta sensu latu*	FAD
		15.89			278.55		*A. ingens*	FAD
		17.15			432.34		*D. maccollumii*	FAD
		17.15			431.98		N. sp. 17 Schrader	FAD
		17.38			736.20		*T. praefraga*	LAD
		17.50			763.84		*T. nansenii*	LAD
		18.85			771.50		*T. praefraga*	FAD
		19.20			432.34		*A. octonarius*	FAD
		24.98			770.50		*T. nansenii*	FAD
AGES FROM FORAMS								
0	0	11.04	83.76	83.8	83.78		*Neogloboquadrina pachyderma*	FAD and LAD
AGES FROM 40Ar-39Ar Dates (±2s errors)								
0.64	0.74	0.691±0.049	10.22	10.24	10.230		Lava clast	
11.17	11.57	11.37±0.20	127.50	127.52	127.510		Pumice lapilli	
10.86	11.92	11.39±0.53	129.96	129.97	129.965		Pumice lapilli	
16.99	17.61	17.30±0.31	640.13	640.16	640.145		Tephra	
17.80	18.50	18.15±0.35	709.14	709.16	709.150		Pumice layer	
17.53	18.33	17.93±0.40	709.17	709.19	709.180		Pumice layer	
18.38	19.04	18.71±0.33	831.66	831.68	831.670		Pumice lapilli	
19.10	19.78	19.44±0.34	953.28	953.31	953.295		Pumice lapilli and dense dark green clasts	
19.15	19.83	19.49±0.34	953.54	953.56	953.550		Pumice lapilli	
19.66	20.36	20.01±0.35	1093.00	1093.04	1093.020		Tephra; Pumice and dense dark clasts	
AGES FROM Sr-Isotope Dates								
10.55	12.95	11.67	144.03	144.06	144.045		1 cm macrofossil (bivalve or barnacle)	
15.75	16.40	16.05	366.80	366.85	366.825		Well preserved, articulated *Adamussium*? sp.	

BIOSTRATIGRAPHY

The biostratigraphy of the AND-2A is discussed in detail in Taviani et al. (this volume). In this section, we focus on the depths of the age diagnostic fossils and biostratigraphic events.

DIATOMS

Most of the diatom events utilized in this initial report are derived from the average composite range model of Cody et al. (2008). Their model is based on a constrained optimization (CONOP) method, which employs a computer-assisted multidimensional correlation technique to interpolate stratigraphic events across different sections resulting in an integrated, high-resolution, quantitative, chronostratigraphic model. Diatom event ages from the average range model are used herein as was done for the AND-1B Core (Wilson et al., 2007). These ages are determined using an approach that allows for the possibility that reworking within the analyzed sections, which is likely in glacial environments, has moved some range ends beyond their original depositional levels. The average range composite model is considered to be most appropriate for preliminary analyses of new drill cores (Cooper et al., 2001; Wilson et al., 2007; Cody et al., 2008). The composite sequence of diatom events produced by Cody et al. (2008) is based on a robust dataset integrating comprehensive diatom biostratigraphy, magnetostratigraphy, and tephrastratigraphy from 32 Neogene sections around the Southern Ocean and Antarctic continental margin as old as 18 Ma. Early Miocene ages for the First Appearance Datum (FAD) and Last Appearance Datum (LAD) of *Thalassiosira nansenii* are from Scherer et al. (2001).

Diatom datums from the AND-2A Core (Tab. 1) provide age constraints down to 772 mbsf. Up-core reworking appears to be insignificant in the diatom-bearing intervals (Taviani et al., this volume). In the upper part of the section, a diatom assemblage that includes the Last Occurrence (LO) and FO of *Thalassiosira elliptipora* (0.64 - 2.06 Ma), LO of *Thalassiosira vulnifica* (2.15 Ma), LO of *Thalassiosira torokina* (2.20 Ma), LO and FO of *Actinocyclus maccollumii* (2.4 - 2.84 Ma), LO of *Thalassiosira inura* (2.53 Ma), and tentatively identified FO of *Rouxia diploneides* (2.55 Ma) (see Taviani et al., this volume) provides an age of 2.06 - 2.84 Ma for the interval 44.06 - 48.24 mbsf. Similarly, three datums – LAD *Denticulopsis lauta* sensu latu (12.46 Ma), LAD *Denticulopsis maccollumii* (14.29 Ma), and FAD *Actinocyclus ingens* (15.89 Ma) – constrain the interval from 225.38 to 278.55 mbsf to be 14.29 - 15.89 Ma. A diatomite unit (310.02 - 312.12 mbsf) is constrained by LAD *Nitzschia* sp. 17 Schrader (15.50 Ma) and the FAD *D. lauta* sensu latu (15.70 Ma) to be between 15.50 and 15.70 Ma. The LAD and FAD of *Thalassiosira praefraga* (17.38 - 18.85 Ma) at 736.20 and 771.50 mbsf, respectively, and the LAD of *T. nansenii* (>17.5 Ma) provide the deepest diatom age constraints.

FORAMINIFERA

The first and last appearance of *Neogloboquadrina pachyderma* occurs in a sample collected from interval 83.76 - 83.80 mbsf. This indicates that the age for this interval must be younger than 11.04 Ma (younger than Chron C5r(y); we use '(y)' to refer to the young end of a chron and '(o)' for the old end).

MACROFOSSILS

The only age diagnostic macrofossil identified was *Adamussium* sp. cf. *A. alanbeui*, which occurs between 999.76 and 999.80 mbsf in LSU 13 and between 1063.71 and 1063.73 mbsf in LSU 14 (Taviani et al., this volume). *Adamussium* sp. cf. *A. alanbeui* has been reported from upper Oligocene to lower Miocene sedimentary units from Antarctica (Taviani & Beu, 2003).

MAGNETOSTRATIGRAPHY

Oriented samples were collected every one to two metres along the core for palaeomagnetic analysis. The paleomagnetic results are discussed in detail in Acton et al. (this volume). A characteristic remanent magnetization (ChRM) with a steep upward direction (normal polarity) or steep downward direction (reversed polarity) was well resolved in 338 of the 695 samples analyzed. These were used to define 23 magnetozones (12 reversed polarity and 11 normal polarity) (Fig. 2; Tab. 1; and Tab. 4 of Acton et al., this volume).

Resolving the ChRM direction and defining magnetozones was difficult above 224.82 mbsf (LSUs 1 through 4) owing to the coarse-grained lithologies, much of which is diamictite, and to the discontinuous sedimentary record. In this interval, only the boundary between magnetozone N1 and R1 (= N1/R1.1), which is most likely the Brunhes/Matuyama (C1n/C1r.1r) reversal (0.781 Ma), provides an age constraint. Given the other age constraints, this reversal could also be one of several other reverse-to-normal transitions less than about 2 Ma, including any of those down to about the C2n/C2r.1r reversal (1.945 Ma). Magnetozone R1.1 (31.10 - 83.56 mbsf) may span one or several reversed polarity chronozones. At least the upper part and perhaps all of it is within the reversed polarity chronozones of the Matuyama (C1r-C2r). However, below the diatom-rich unit at 48 mbsf, the magnetozone could be correlated to any reversed polarity chronozone from about C2r.2r to C5r (2.148 - 12.014 Ma). Independent age constraints are very poor down to the base of LSU 4. Thus, magnetozone R1.2 (96.80 - 115.71 mbsf) could also be correlated to any reversed polarity chronozone from about Chron C2r.2r to C5r.

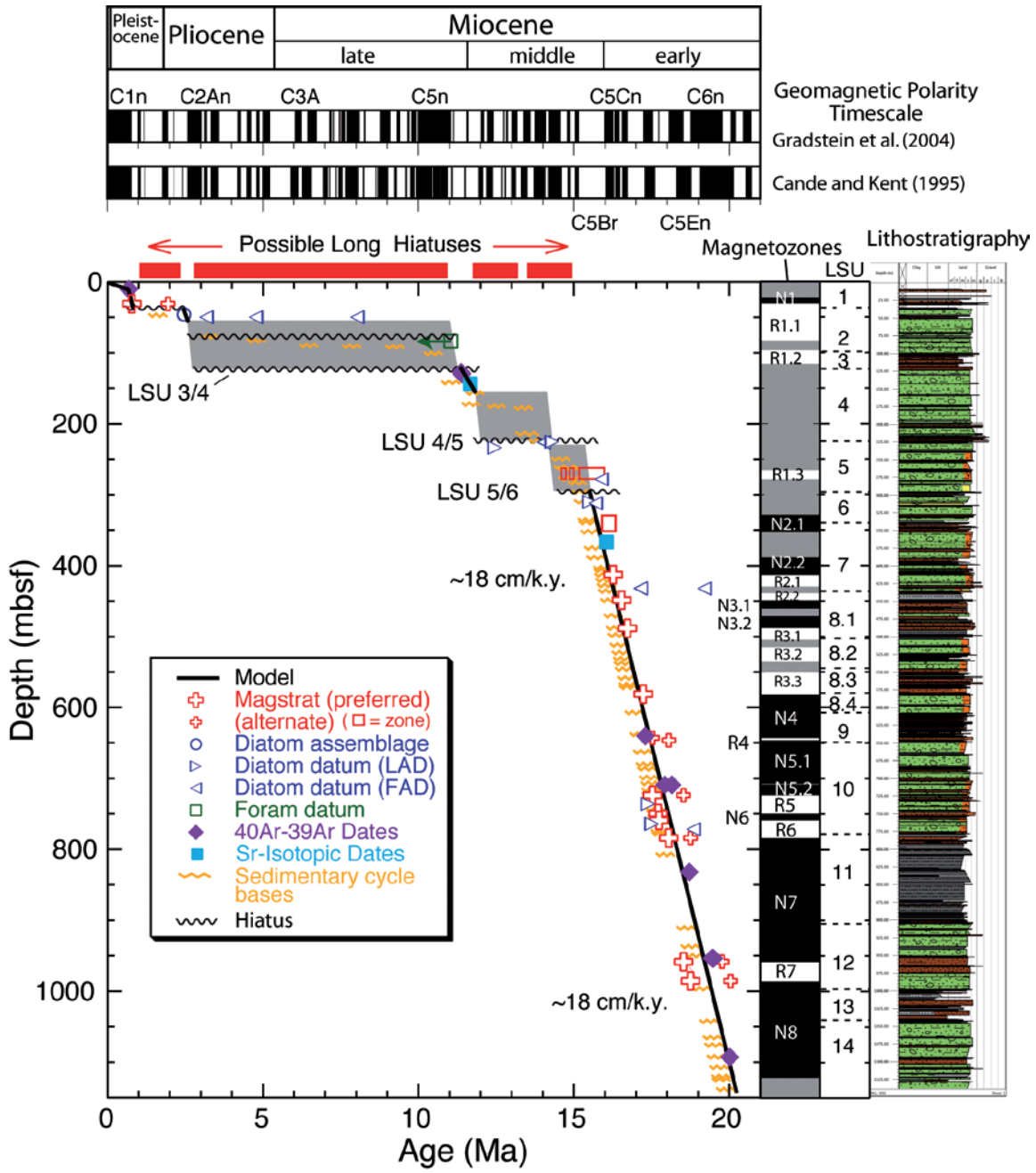

Fig. 2 - Age-model for AND-2A (see Tab. 1). The preliminary magnetic polarity stratigraphy is plotted to the right of the Age-vs.-Depth diagram. The black intervals are normal polarity, the white intervals are reversed polarity, and the gray intervals are uncertain polarity. The summary lithologic column is plotted on the far right. The black and white bar running along the top of the plot is the geomagnetic polarity timescale the Gradstein et al. (2004) and Cande and Kent (1995), with selected chrons labeled.

From LSUs 5 through 7, the magnetozones are again identified mainly within broader zones of uncertain polarity. These magnetozones can be correlated to the geomagnetic polarity timescale (GPTS) using the independent age constraints provided by other data, but provide only weak additional age information. Sedimentation is more continuous below the LSU 4/5 boundary and the sedimentation rates are high, which aids in interpreting the magnetozones. Given these constraints, magnetozone R1.3 (265.55 - 278.48 mbsf) probably correlates to Chron C5Br (15.160 - 15.974 Ma) but could also be C5ADr (14.581 - 14.784 Ma) or C5Bn.1r (14.877 - 15.032 Ma). Magnetozones N2.1 (328.52 - 352.15 mbsf) and N2.2 (388.50 - 413.26 mbsf) probably correlate to the younger and older parts of Chron C5Cn.1n (15.974 - 16.268 Ma), respectively.

Below the LSU 7/8 contact (436.18 mbsf), the quality of paleomagnetic results improves considerably and provides a continuous polarity stratigraphy for this interval (Acton et al., this volume). The sequence of magnetozones from R2.1 through R3.3 (413.26 - 581.34 mbsf) correlates with Chrons C5Cr.1r through C5Cr (16.268 - 17.235 Ma). Below this, magnetozones N4 through N8 (643.02 mbsf to the base of the hole) can be correlated with either Chrons C5Dn through C6n (our preferred interpretation), or with Chrons C5Dn through C6An.1n (an alternate interpretation). If our preferred interpretation is correct, the ages for the magnetozone boundaries are slightly younger than

Tab. 2 - Samples collected from Core AND-2A for ^{40}Ar-^{39}Ar dating.

Sample Number	*Top Depth*	*Bottom Depth*	*Lithology*	*Date samples were collected*
	(mbsf)	*(mbsf)*		
1	10.22	10.44	lava clast	15 October 2007
2	12.23	12.41	lava clast	15 October 2007
4	18.03	18.25	basaltic lava flow	17 October 2007
3	18.69	18.73	lava clast	15 October 2007
5	86.69	86.71	pumice lapilli	22 October 2007
6	92.62	92.64	scattered pumices*	24 October 2007
7	93.11	93.13	pumice lapilli*	24 October 2007
8	93.18	93.20	pumice lapilli*	24 October 2007
9	127.50	127.52	pumice lapilli	25 October 2007
10	129.96	129.97	pumice lapilli	25 October 2007
11	131.97	131.99	pumice lapilli	25 October 2007
12	188.26	188.30	pumice lapilli	27 October 2007
13	420.97	420.98	pumice lapilli*	8 November 2007
14	443.65	443.67	pumice lapilli*	9 November 2007
15	564.88	564.90	lava clast	13 November 2007
16	597.70	597.72	pumice lapilli	13 November 2007
17	640.13	640.16	ash layer	15 November 2007
18	709.14	709.16	pumice layer	17 November 2007
19	709.17	709.19	pumice layer	17 November 2007
20	831.66	831.68	pumice lapilli accumulation	22 November 2007
21	953.28	953.31	pumice lap. and dark dense clasts	25 November 2007
22	953.54	953.56	pumice lapilli accumulation	25 November 2007
23	1093.00	1093.04	scattered pumice lapilli and dark dense clasts	30 November 2007

* indicates that insufficient material was available for dating

indicated by the radioisotopic dates. Alternatively, if the magnetozones are Chrons C5Dn-C6An.1n, the ages for the magnetozone boundaries are slightly older than indicated by the radioisotopic dates. This assumes the ages given for the chrons in the Gradstein et al. (2004) GPTS are correct. The Cande and Kent (1995) GPTS gives slightly older ages for Chrons C5D through C6A, which would make our preferred correlation more compatible with the radioisotopic dates.

In both cases, the thicknesses of the reversed polarity zones relative to the normal polarity zones are somewhat less than expected from the GPTS if sedimentation rates had been relatively constant at Site AND-2A. This is particularly the case for the alternative interpretation as the very thin magnetozone R4 would correlate to C5Dr. In our preferred interpretation, magnetozone R4 is instead an excursion within Chron C5Dn. Sedimentation rates are unlikely to be constant, so neither interpretation can be eliminated based only on the relative thickness of the magnetozones.

^{40}Ar-^{39}Ar GEOCHRONOLOGY

A total of 23 samples were selected during on-ice activities for subsequent radioisotopic age determination (Tab. 2; Fig. 2). Twelve of the samples were collected from the upper 200 mbsf, with most of these being volcanic clasts embedded in diamictite. Given the good state of preservation of some of these clasts, their ages should be similar to that of the diamictite in which they were entrained. Selected samples were examined and ten of them were determined to contain sufficient material for ^{40}Ar-^{39}Ar dating. In May 2008, additional clast samples were collected from the upper 200 m and from 358, 441 and 565 mbsf. These samples will be the focus of future studies. No datable material was collected between 200 and 358 mbsf. Eleven samples were collected below 565 mbsf, including samples from an ash layer with potassium-rich feldspar crystals at 640.16 mbsf. Most of the other samples are pumice lapilli and clasts, including a tephra sample from 1093.0 mbsf, which is near the base of the AND-2A sequence.

Radioisotopic dating was done at IGG-CNR in Pisa, Italy, using a noble gas mass spectrometer (MAP215-50) equipped with a low-volume stainless steel inlet system and using laser extraction techniques (Nd:YAG and CO_2 lasers). So far, 10 of the 23 samples have been dated. Uncertainties quoted are full 2σ errors that include analytical errors, uncertainties in neutron fluence, monitor age and ^{40}K decay constants.

The youngest radioisotopic age (0.691±0.049 Ma) was obtained from a volcanic clast from a volcanic breccia at 10.22 mbsf. Two lava clasts from 127 - 130 mbsf in LSU 4 give statistically indistinguishable ages, indicating that this part of LSU 4 is ~11.3 - 11.4 Ma. This supports the foraminiferal datum from 83.76 mbsf, which indicated an 11 Ma maximum age for this part of LSU 2. All three ages are further supported by a Sr-isotope date of ~11.7 Ma at 144.03 mbsf in LSU 4. An ash layer in the middle of the section (640 mbsf) gives an age of 17.30±0.31 Ma. Two samples from 953 mbsf and the sample from 1093 mbsf provide

age constraints that suggest the oldest sediments cored in Hole AND-1A are about 20 Ma (Tab. 1). The radioisotopic ages along with the other age constraints indicate that AND-2A contains a very thick lower Miocene record from 1138 to about 380 mbsf, a thick middle Miocene record from about 380 mbsf to near the top of LSU 4 (probably to about 140 mbsf; where the middle Miocene is 11.61 - 15.97 Ma as defined by Gradstein et al. (2004)), and an upper Miocene to Recent section above this.

Sr-ISOTOPE DATING

Most macrofossils recovered in the upper 125 m are decalcified, making them unsuitable for Sr isotopic dating. Five samples were collected in this interval, with three of them coming from a narrow interval (67 - 68 mbsf) (Tab. 3; Fig. 3). Macrofossil abundance increases downhole and the state of preservation improves. A total of 14 samples were collected from 144 mbsf to the total depth of the hole, with seven of these coming from the interval 416 - 431 mbsf.

All analyses were carried out at the University of Michigan. Elemental ratios (Mg/Ca, Sr/Ca, Mn/Ca and Fe/Ca) were acquired using a ThermoFisherFinnigan Element inductively coupled plasma-mass spectrometer (ICP-MS). The method was modified from that used by Rosenthal et al. (1999). Analytical precision was better than 2% for Ca, 1% for Sr and 5% for Mn and Fe relative standard deviation (%RSD) based on check standards, laboratory reference material, and sample replicates.

For the Sr isotopic investigations, the extra solution from ICP-MS measurements was left to evaporate before being redissolved in 2.5N HCl. Separation of Sr from the other elements by column chromatography, followed the procedures outlined by Mukasa et al. (1991). Each sample was dried to a solid, treated with a drop of 14N HNO_3, redried, and then loaded with a 0.1% H_3PO_4 and $TaClO_4$ solution on a single rhenium filament. These samples were run on a multi-collector TIMS "VG Sector". Strontium isotope composition was corrected for mass-fractionation using $^{86}Sr/^{88}Sr=0.1194$. The repeated analyses of NBS-987 standard gave an average ratio of $^{87}Sr/^{86}Sr=0.710251\pm10$ (n=4). Total blanks averaged 0.35 ng for Sr, which are negligible. Ages were obtained as described in Howarth and McArthur (1997) and McArthur et al. (2001) applying the Look-up Tables Version 4:08/04. Error bars include uncertainty from both the isotope determinations and the 95% confidence levels on the age curve.

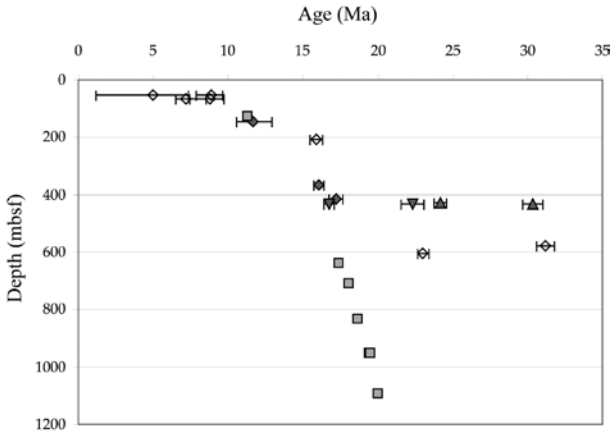

Fig. 3 - Plot of preliminary $^{87}Sr/^{86}Sr$ (rhombs) and ^{40}Ar-^{39}Ar (squares) ages against depth. Sr-isotopic age symbols are coded according to material preservation as revealed by elemental chemistry and cathodoluminescence analysis. Open rhombs represent samples that show clear indications of diagenetic alteration, while filled ones represent fragments that show marginal or no signs of diagenetic alteration. The triangles are two aragonite samples that produced unreasonably old ages. The inverted triangles at the same depth of the aragonites come from a single sample with mixed material that requires further discrimination.

Tab. 3 - Samples collected from Core AND-2A for Sr-isotopic dating.

Sample Depth (mbsf)	*Sample information*
53.51-53.52	indeterminate microfossil fragment, barnacle?
67.13-67.15	indeterminate macrofossil, chalky
67.47-67.50	indeterminate ornamented bivalve? (1cm), chalky
67.56-67.59	indeterminate macrofossil,chalky
122.96-122.98	indeterminate macrofossil frag, chalky
144.03-144.06	1 cm macrofossil (bivalve or barnacle)
175.41-175.43	serpulid tubes relatively well preserved
208.96-208.99	pectinid frags; indeterminate bivalve? frag
366.80-366.85	well preserved, articulated *Adamussium*? sp.
416.78-416.79	indeterminate bivalve frag, thick (pectinid?)
428.44-428.46	Veneridae sp.1, well preserved but sliced
429.28-429.30	Veneridae sp.1, well preserved but sliced
429.30-429.33	thick pectinid? frag
430.41-430.48	Barnacle >1cm, relatively fresh; frags
430.49-430.51	Veneridae sp.1, well preserved, sectioned
430.54-430.68	Costate pectinid, articulated; well preserved
576.29-576.32	serpulid tubes
605.61-605.66	Costate pectinid, well preserved shell, sliced
1063.71-1063.73	*Adamussium* cf. *alanbeui*, well preserved, with umbo, sliced

Preliminary cathodoluminescence and elemental analyses on 14 of the 19 samples confirmed that diagenetic alteration, though notable in some intervals, is not a pervasive problem downcore. For this first set of samples, Sr-isotope analysis was done on all pieces despite signs of incipient alteration. Ages based on the $^{87}Sr/^{86}Sr$ of diagenetically altered samples of all fragment types were consistently older than other age indicators (Fig. 3).

Unaltered material came from pectinid and venerid bivalves. Two samples, one from an *Adamussium* sp. shell fragment and the other from a costate pectinid shell fragment, provided ages coincident with other age estimates (Tab. 1; Fig. 2). Venerid pieces, which appear to be aragonitic (based on chemical makeup and XRD profiles), produced older ages than expected. The ages obtained from aragonitic fragments (as opposed to the pectinid ones) that appear to be too old are the focus of ongoing research.

The observed unaltered chemical profiles and the $^{87}Sr/^{86}Sr$ ages obtained so far suggest that it should be possible to provide additional age constraints on at least some sections of the core with more Sr isotopic determinations. Once all preliminary analyses are completed, other samples will be selected and micro-sampled using what was learned from this initial set. Effective sample discrimination will increase chances of success while minimizing material destruction.

ASTRONOMICAL TUNING

The occurrence of orbitally induced variations in physical, magnetic, and chemical properties of stratigraphic sections provides another manner for dating geologic units. Currently, it is too early to say whether orbital cyclicity exists in the AND-2A record because signal analysis studies are just getting underway. Various parameters (lithology, XRF elements, physical properties, magnetic parameters) do, however, show features that are suggestive of cyclicity in some sections of the AND-2A core. For example, LSU 4 has a clear signal with a wavelength of ~20 meters. Similarly, the susceptibility has a long wavelength variation of ~100 to 200 meters from the base of the hole up to ~700 mbsf. The chronostratigraphic significance of these cycles will need to be tested once better age constraints are established and hiatuses and discontinuities have been identified and/or confirmed.

REGIONAL AND GLOBAL CORRELATION

Correlation of physical, magnetic, and chemical properties, key seismic reflectors, and lithologic variations of the AND-2A core with dated proxy records from regional or distant locations provides another viable dating method. Currently, only tentative correlations have been made using lithologic and seismic correlation to other drill sites in the Ross Sea region (Fielding et al., 2006, 2008) and are discussed in the synthesis paper (Harwood et al., this volume).

EROSIONAL SURFACES

Numerous erosional contacts were noted in the core (Fielding et al., this volume) and probably many others occur within some of the glacial deposits but are difficult to identify visually. Some of these undoubtedly correspond to significant hiatuses, particularly in the upper four lithostratigraphic units.

Only where dates could be obtained for the sediments above and below these contacts, could we accurately assess the amount of time missing at each contact. Unfortunately, datable material does not occur continuously throughout the sedimentary succession on a scale that allows a rigorous and precise assessment of actual time missing. Current chronostratigraphic data do allow us to recognize that time is missing in the section and that the time missing is relatively insignificant at some erosional surfaces and significant (hundreds of thousands to millions of years) at others.

Forty one glacial surfaces of erosion were included in the age model developed for the AND-1B core (Wilson et al., 2007). We follow a similar strategy for AND-2A by including the location of 71 probable contacts between sedimentary cycles. C.R. Fielding and colleagues have identified these 71 cycle boundaries in a preliminary sequence stratigraphic model that is currently being developed. Most of these sedimentary intervals represent glacial and eustatic cycles although tectonic processes have likely influenced the depositional character of some of the units. We used the cycle boundaries (plotted in Fig. 2) to guide placement of major hiatuses as we constructed the age model.

AGE MODEL AND SEDIMENTATION RATES

The combined, preliminary age constraints are given in table 1 and plotted in figure 2. These ages indicate that the sedimentary section is comprised of a fairly continuous and thick lower and middle Miocene section below 224.82 mbsf and a discontinuous middle/upper Miocene to Recent section above this. The upper portion of the section contains multiple hiatuses resulting from the discontinuous nature of deposition and common erosional episodes that are typical of environments at the margin of a dynamic ice sheet.

We construct an age model that fits the current age constraints and that incorporates several major hiatuses. One or more of these breaks in the record are located between 50 and 122.86 mbsf, with an accumulative loss of over 7 m.y. We cannot delineate a precise location for the hiatus or hiatuses within this interval but schematically illustrate two options

in figure 2 with the uppermost hiatus occurring at the base of a glacial cycle at 77.66 mbsf and the lowermost hiatus occurring at the LSU 3/4 boundary (122.86 mbsf). The sediment ages within this interval can only be imprecisely dated as being between about 3 and 11 Ma. An additional hiatus that is approximately 3 m.y. in duration is placed at 224.82 mbsf (the LSU 4/5 boundary). This break in the record could actually be accommodated on multiple erosional/non-depositional surfaces that occur between 145 mbsf and the LSU 4/5 boundary (224.82 mbsf) but, at present, this is an interval without age constraints.

Ages within LSU 5 are constrained to be between about 14.2 Ma (the absence of *D. simonseni* and the LAD *D. maccollumii* from the top of LSU 5) and 15.7 Ma (FAD *D. lauta* sensu latu near the top of LSU 6). The sedimentation rate is therefore at least 4.7 cm/k.y. but is more likely much higher than this and one or more hiatuses occur within LSU 5 or at the LSU 5/6 boundary.

Below the LSU 5/6 boundary (296.34 mbsf), sedimentation was relatively continuous and rapid and the age model is well constrained by 9 diatom datums, seven ^{40}Ar-^{39}Ar dates, one Sr-isotope date, and 19 magnetozones. Even so, short hiatuses (less than a few hundred thousand years) undoubtedly occur but are beyond the resolution of the chronostratigraphic age constraints.

Although the linear age model for the interval from 296.34 - 1138.54 (Fig. 2) is an over simplification of the true ages of the sediments, it serves to illustrate the point that sedimentation was relatively continuous over much of the early and middle Miocene at Site AND-2A. Numerous more complex age models could be derived from the age constraints but such models would not necessarily be more accurate. A more accurate representation would likely involve placing at least short hiatuses on observed erosional contacts, but the number and significance of these contacts are still under investigation.

The 'relatively' continuous and rapid nature of deposition is supported by diatom datums, which provide particularly good age control from LSU 6 down to 771.5 mbsf (in LSU 10), where the FO of *T. praefraga* (18.85 Ma) is observed. These datum ages are supported by radioisotopic dates of 17.30±0.31 Ma at 640.14 mbsf (in LSU 9) and 18.15±0.35 and 17.93±0.40 Ma for samples from 709.15 and 709.18 mbsf (in LSU 10), respectively, and 18.71±0.33 Ma for a sample from 831.67 mbsf (in LSU 11).

The sediments from 783.69 mbsf to the base of the hole comprise two thick normal polarity magnetozones that bound a thinner reversed polarity magnetozone (958.59 - 985.64 mbsf). This polarity sequence is most likely Chrons C5En, C5Er, and C6n, which spans 18.056 - 19.772 Ma using the timescale of Gradstein et al. (2004) or slightly older (18.281 - 20.121 Ma) using the Cande and Kent (1995) timescale. Alternatively, the sequence could be Chrons C6n, C6r, and C6An.1n (18.748 - 20.213 Ma), although this interpretation gives ages older than most of the radiometric dates.

Based on this preliminary age model, the mean sediment accumulation rate is ~18 cm/k.y. from the top of LSU 6 to the base of the hole (Fig. 2). This represents an interval average rather than true sediment accumulation rates, which could be quite variable. Sediment accumulation rates within LSUs 1 through 5 are difficult to constrain given the discontinuous nature of sedimentation, but are likely to include intervals of rapid deposition punctuated by hiatuses.

Acknowledgements – We thank the SMS curatorial staff for their professional handling of the core and for administering the many sample requests, the SMS Project drill crew for their expertise in recovering the core, and to the funding agencies in the USA, New Zealand, Italy, and Germany that provided the financing for the ANDRILL SMS Project. The ANDRILL Program is a multinational collaboration between the Antarctic programs of Germany, Italy, New Zealand and the United States. Antarctica New Zealand is the project operator and developed the drilling system in collaboration with Alex Pyne at Victoria University of Wellington and Webster Drilling and Exploration Ltd. Antarctica New Zealand supported the drilling team at Scott Base; Raytheon Polar Services Corporation supported the science team at McMurdo Station and the Crary Science and Engineering Laboratory. The ANDRILL Science Management Office at the University of Nebraska-Lincoln provided science planning and operational support. Scientific studies are jointly supported by the US National Science Foundation (NSF), NZ Foundation for Research, Science and Technology (FRST), the Italian Antarctic Research Programme (PNRA), the German Research Foundation (DFG) and the Alfred Wegener Institute for Polar and Marine Research (AWI).

REFERENCES

Acton G., Florindo F., Jovane L., Lum B., Ohneiser C., Sagnotti L., Strada E., Verosub K.L., Wilson G.S., & the ANDRILL-SMS Science Team, 2008-2009. Palaeomagnetism of the AND-2A Core, ANDRILL Southern McMurdo Sound Project, Antarctica. *Terra Antartica*, **15**, this volume, 193-210.

Cande S.C. & Kent D.V., 1995. Revised Calibration of the Geomagnetic Polarity Timescale for the Late Cretaceous and Cenozoic. *J. Geophys. Res.*, **100**, 6093-6095.

Cody R.D., Levy R.H., Harwood D.M. & Sadler P.M., 2008. Thinking Outside the Zone: High-Resolution Quantitative Biochronology for the Antarctic Neogene. *Palaeogeography, Palaeoecology, Palaeoclimatology*, **260**, 92-121.

Cooper R.A., Crampton J.S., Raine J.I., Gradstein F.M., Morgans H.E.G., Sadler P.M., Strong C.P., Waghorn D. & Wilson G.J., 2001. Quantitative Biostratigraphy of the Taranaki Basin, New Zealand: a Deterministic and Probabilistic Approach. *AAPG Bull.*, **85**, 1469-1498.

Fielding C.R., Henrys S.A. & Wilson T.J., 2006. Rift history of the western Victoria Land Basin: a New Perspective Based on Integration of Cores with Seismic Reflection Data. In: D.K. Futterer, D. Damaske, G. Kleinschmidt, H. Miller & F. Tessensohn, (eds.), *Antarctica: Contributions to Global Earth Sciences*, Springer-Verlag, Berlin, 309-318.

Fielding C.R., Whittaker J., Henrys S.A., Wilson T.J. & Naish T.R., 2008. Seismic Facies and Stratigraphy of the Cenozoic Succession in McMurdo Sound, Antarctica: Implications for Tectonic, Climatic and Glacial History. *Palaeogeography, Palaeoclimatology, Palaeoecology*, **260**, 8-29.

Fielding C.R., et al. & the ANDRILL-SMS Science Team,2008-2009. Sedimentology and Stratigraphy of the AND-2A Core, ANDRILL Southern McMurdo Sound Project, Antarctica. *Terra Antartica*, **15**, this volume, 77-112.

Gradstein F.M., Ogg J. & Smith A.G, 2004. *A Geologic Time Scale 2004*. Cambridge University Press, Cambridge, United Kingdom, 610 pp.

Howarth R.J. & McArthur J.M., 1997. Statistics for Strontium Isotope Stratigraphy. A Robust LOWESS Fit to the Marine Sr-isotope Curve for 0 - 206 Ma, with Look-up Table for the Derivation of Numerical Age. *J. Geol.*, **105**, 441-456.

McArthur J.M., Howarth R.J. & Bailey T.R., 2001. Strontium Isotope Stratigraphy: LOWESS Version 3. Best-fit Line to the Marine Sr-isotope Curve for 0 to 509 Ma and Accompanying Look-up Table for Deriving Numerical Age. *J. Geol.*, **109**, 155-169.

Mukasa S.B., Shervais J.W., Wilshire H.G. & Nielson J.E., 1991. Intrinsic Nd, Pb, and Sr Isotopic Heterogeneities Exhibited by the Lherz Peridotite Massif, French Pyrenees. *J. Petrol. Spec. Lith. Issue,* 117-134.

Rosenthal Y.M., Field M.P. & Sherrell R.M., 1999. Precise Determination of Element/calcium Ratios in Calcareous Samples Using Sector Field Inductively Coupled Plasma Mass Spectrometry, *Analytical Chemistry*, **71**, 3248–3253.

Scherer R.P., Bohaty S.M. & Harwood D.M., 2001. Oligocene and lower Miocene siliceous microfossil biostratigraphy of Cape Roberts Project Core CRP-2/2A, Victoria Land Basin, Antarctica. In: P.J. Barrett & C.A. Ricci, (eds.). Studies from the Cape Roberts Project, Ross Sea, Antarctica, Scientific Report of CRP-2/2A, *Terra Antartica*, **7**, 417-442.

Naish T. & the ANDRILL-MIS Science Team, 2007. Synthesis of the Initial Scientific Results of the MIS Project (AND-1B Core), Victoria Land Basin, Antarctica, *Terra Antartica*, **14**(3), 317-327.

Taviani M. & Beu A.G., 2003. The Paleoclimatic Significance of Cenozoic Marine Macrofossil Sssemblages from Cape Roberts Project drillholes, McMurdo Sound, Victoria Land Basin, East Antarctica. *Palaeogeography, Palaeoclimatology, Palaeoecology*, **198**, 131-143.

Taviani M., et al. & the ANDRILL-SMS Science Team, 2008-2009. Palaeontological characterization and analysis fo the AND-2A Core, ANDRILL Southern McMurdo Sound Project, Antarctica. *Terra Antartica*, **15**, this volume, 113-146.

Wessel P., and Smith, W.H.F., 1998, New, Improved Version of the Generic Mapping Tools Released, *EOS Trans. AGU*, **79**, 579.

Wilson G., Levy R., Browne G., Cody R., Dunbar N., Florindo F., Henry S., Graham I., McIntosh W., McKay R., Naish T., Ohneiser C., Powell R., Ross J., Sagnotti L., Scherer R., Sjunneskog C., Strong C.P., Taviani M., Winter D. & the ANDRILL-MIS Science Team, 2007. Preliminary Integrated Chronostratigraphy of the AND-1B Core, ANDRILL McMurdo Ice Shelf Project, Antarctica. *Terra Antartica*, **14**, 297-316.